

ESTIMATING THE MULTIPATH STRUCTURE OF AN UNDERWATER CHANNEL USING A SINGLE VECTOR SENSOR

Paulo Felisberto LARSyS, University of Algarve, PT
Orlando Rodríguez
Sérgio Jesus

1 INTRODUCTION

Model based estimation of source positioning and other ocean parameters using a broadband signal and a single hydrophone has been addressed by several authors [1–4]. Single hydrophone systems are low cost and it can be easily installed in small platforms. However, model based estimation methods require a large number of time consuming forward model runs associated with complex optimization procedures, that are not suitable for real-time low-end computational systems. Vector sensors are devices that in addition to acoustic pressure measured by conventional hydrophones, measure particle velocity that gives directional information of the acoustic field. The intrinsic spatial filter capabilities of vector sensors were widely investigated to improve direction of arrival estimation after Nehorai and Paldi work [5]. This work in addition to vector sensor array methods proposed a single vector sensor method based on intensity measurements that allows to estimate azimuth and elevation of a source in an unbounded environment. Felisberto et al. [6] shown with field data that the method can be used in a shallow water environment to estimate the source azimuth. However, due to multipath the method can not be used to estimate the elevation angle. Hawkes and Nehorai [7] proposed a method to estimate the elevation of the direct echo impinging a receiver close to the bottom by mitigation the influence of the bottom reflected echo. In this work a different approach is followed: the elevation of the various echoes impinging the vector sensor are estimated from the amplitude of the their particle velocity components by least squares with the respective time delays. Using this information rays are backpropagated to localize the source in range and depth. This two step method can be implemented with a single forward raytracing model run, thus is very fast and suitable to light systems.

The paper is organized as follow: the vector sensor measurement model is provided in Section 2, the two step range-depth estimation method is depicted in Section 3, the simulation results are discussed in Section 4. Finally, in Section 5 the main conclusions are drawn.

2 MEASUREMENT MODEL

In the following it is assumed that there is a point acoustic source emitting the signal $s(t)$. The signal is received by a vector sensor composed by 3 orthogonal particle velocity sensors, two aligned with the horizontal plan, $v_x(t)$ and $v_y(t)$, and one in the vertical plane $v_z(t)$. The particle velocity is the gradient of the pressure $p(t)$ at a given point, thus considering that the source is in the farfield of a free-space environment with density ρ_0 and sound speed c , the dimension of the vector sensor is small compared with wavelength, then the wavefront impinging is planar, the pressure and particle velocity components are related by [7]

$$\begin{bmatrix} v_x(t) \\ v_y(t) \\ v_z(t) \end{bmatrix} = \alpha p(t) \begin{bmatrix} u_x \\ u_y \\ u_z \end{bmatrix} \quad (1)$$

where α is a proportionality constant and u_x, u_y, u_z are components of the unit vector \mathbf{u} at the vector sensor pointing towards the source.

In an underwater multipath environment, a convenient model to represent the pressure field $p(t)$ due to M echoes impinging a receiver far away from the boundaries is given by

$$p(t) = \sum_{m=1}^M a_m s(t - \tau_m) + n_p(t) \quad (2)$$

where a_m is the strength of the different echoes and τ_m the respective time delays. n_p represents the additive noise. This model can be extended to the particle velocity field by

$$\begin{bmatrix} v_x(t) = \sum_{m=1}^M a_m^x s(t - \tau_m) + n_x(t) \\ v_y(t) = \sum_{m=1}^M a_m^y s(t - \tau_m) + n_y(t) \\ v_z(t) = \sum_{m=1}^M a_m^z s(t - \tau_m) + n_z(t) \end{bmatrix} \quad (3)$$

where the coefficients a_m^x, a_m^y, a_m^z are the attenuation along the m -th path for the 3 components of the particle velocity. The noise sequences $n_x(t), n_y(t), n_z(t)$ are additive and uncorrelated with the signal. Moreover, it is assumed that noise sequences are uncorrelated, what is a fair assumption when the sensor self-noise is the most relevant noise component. Making the further assumption that the signal $s(t)$ is known and has a narrow autocorrelation, least-square or maximum likelihood approach for time delay and amplitude estimation [2] can be applied. Given the estimates of a_m^x, a_m^y, a_m^z , the estimates of the elevation (and azimuth) of the different echoes can be obtained by simple relations.

3 SOURCE POSITIONING ESTIMATION METHOD

The proposed method to estimate the source positioning in azimuth, range and depth is depicted in next subsections. The estimation of the azimuth of a single source can be implemented using fast and low computational demanding intensity based algorithms [6]. Herein the focus is on range-depth source localization in the source-receiver plane, that combined with the azimuth gives a full estimation of the source position. The range-depth estimation procedure has two steps. In a first step the number of angles of the echoes that impinges the array are estimated, then using the angles information, rays are backpropagated to estimate the source-range and depth.

3.1 AMPLITUDE-DELAY-ANGLE ESTIMATION

Considering a snapshot of N samples acquired at a sampling period Δt , the system Eq.(3) can be write as

$$\mathbf{Y} = \mathbf{S}(\tau)\mathbf{A} + \mathbf{N} \quad (4)$$

where \mathbf{Y} is a matrix of dimension $N \times 3$, which columns $\mathbf{v}_x, \mathbf{v}_y, \mathbf{v}_z$ represent the components of the vector sensor ($\mathbf{Y} = [\mathbf{v}_x | \mathbf{v}_y | \mathbf{v}_z]$), amplitude matrix \mathbf{A} is of dimension $M \times 3$, $\mathbf{A} = [\mathbf{a}_x | \mathbf{a}_y | \mathbf{a}_z]$, $\mathbf{a}_x, \mathbf{a}_y, \mathbf{a}_z$ are the vectors of amplitudes of individual components. The matrix $\mathbf{S}(\tau)$ is a matrix of dimension $N \times M$ ($\tau = [\tau_1, \dots, \tau_m, \dots, \tau_M]$), where the m -th column is given by $\mathbf{s}(\tau_m) = [s(-\tau_m), \dots, s((N-1)\Delta t - \tau_m)]^T$. The matrix \mathbf{N} of dimension $(N \times 3)$ represent the noise components ($\mathbf{N} = [\mathbf{n}_x | \mathbf{n}_y | \mathbf{n}_z]^T$).

If the amplitude matrix \mathbf{A} is deterministic, the least squares approach can be used to estimate the amplitudes and time delays [2]. Assuming that the delays are known the amplitudes are estimated by minimizing the functional

$$\hat{\mathbf{A}} = \arg\{\min_{\mathbf{A}} \|\mathbf{Y} - \mathbf{S}(\tau)\mathbf{A}\|^2\}, \quad (5)$$

which solution is given by

$$\hat{\mathbf{A}}(\tau) = (\mathbf{S}^H(\tau)\mathbf{S}^{-1}(\tau)\mathbf{S}^H(\tau)\mathbf{Y}) \quad (6)$$

where \mathbf{H} represents the complex conjugate transpose. Since the time delays are generally unknown, the amplitudes are estimated for each plausible time delay giving rise to a delay-amplitude curve. The

envelope of the absolute value of a delay-amplitude curve is known as arrival pattern. The amplitude-delay estimates of the echoes are given by its M highest peaks (absolute value). When the noise is white and the different echoes suffer uncorrelated perturbations the amplitude-delay estimated procedure can be equivalently obtained by matched filter. Once the coefficients of m -th echo are estimated $\hat{a}_m^x, \hat{a}_m^y, \hat{a}_m^z$, then the corresponding azimuth and elevation $\hat{\theta}_m, \hat{\phi}_m$ are given by

$$\hat{\theta}_m = \arctan \frac{\hat{a}_m^y}{\hat{a}_m^x}, \quad (7)$$

$$\hat{\phi}_m = \arctan \frac{\hat{a}_m^z}{\sqrt{(\hat{a}_m^x)^2 + (\hat{a}_m^y)^2}}. \quad (8)$$

However, considering a single sound source the azimuth of different echoes impinging the vector sensor are the same which can be estimated more efficiently using an intensity based algorithm [6]. Next, the elevation estimates of the different echoes with the respective time delays will be used to estimate the range-depth source localization.

3.2 RANGE-DEPTH ESTIMATION

The source range and depth backpropagation estimation procedure used in this work was introduced by Voltz and Lu [8]. Considering an hypothetic ideal acoustic channel without noise where one is able to determine the elevation of the echoes impinging the array and associated arrival times, and in addition, one has at hand a ray propagation code that accurate model the rays trajectories. By the reciprocity principle a ray launched from the receiver location at a given angle, has the same trajectory as an echo received at this elevation angle. One say that such a ray is backpropagated. Tracing the trajectories of at least 2 echoes impinging a receiver from different elevation angles the possible source location (range-depth) are in points where all the considered trajectories intersect. Several intersection points could occur along the trajectories, however using the knowledge of relative time delays between echoes the source position can be unequivocally determined. It can be done by time aligning the different rays, i.e. delaying rays by the estimated relative delays. Plotting the trajectories of the source localization can be obtained by visual inspection, however it can be posed as a minimization problem, by defining the mean range $\bar{r}(\tau_a)$ and the mean depth function $\bar{z}(\tau_a)$

$$\bar{r}(\tau_a) = \frac{1}{M} \sum_{m=1}^M r_m(\tau_a) \quad (9)$$

$$\bar{z}(\tau_a) = \frac{1}{M} \sum_{m=1}^M z_m(\tau_a) \quad (10)$$

where τ_a is the aligned time, $r_m(\tau_a)$ and $z_m(\tau_a)$ are respectively the range and depth in m -th ($m = 1 \dots M$) ray trajectory. The range-depth localization is obtained by join minimizing the range variance $\sigma_r^2(\tau)$ and the depth variance $\sigma_z^2(\tau_a)$ given by

$$\sigma_r^2(\tau_a) = \frac{1}{M} \sum_{m=1}^M (r_m(\tau_a) - \bar{r}_m(\tau_a))^2, \quad (11)$$

$$\sigma_z^2(\tau_a) = \frac{1}{M} \sum_{m=1}^M (z_m(\tau_a) - \bar{z}_m(\tau_a))^2. \quad (12)$$

In the ideal case both variances reach 0 at the source true localization. In realistic case the same approach can be considered, but the objective function to be minimized is the sum of both variances, i.e.

$$\sigma^2(\tau_a) = \sigma_r^2(\tau_a) + \sigma_z^2(\tau_a) \quad (13)$$

or equivalently the standard deviation σ .

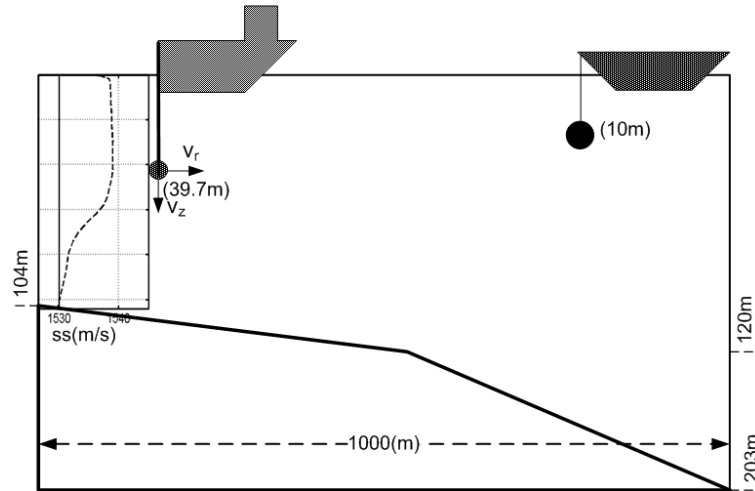


Figure 1: MAKAI'05 environmental scenario used for the simulation

4 SIMULATION RESULTS

Herein is presented a simulation example to test the methods described in the previous sections. The simulation scenario (Fig. 1) is based on the MAKAI'05 field calibration experiment [9], where a 4 element vector sensor array was suspended from a research vessel at depth 39.6 m (in this simulation only the vector sensor at this depth is considered). The receiver position is considered fixed. The sound source was suspended at 10 m water depth, transmitted a LFM sweep with duration 50 ms and frequency band 8–14kHz at various positions between 100 m and 1000 m from the receiver. The bathymetry is range dependent with water depth 104 m at receiver range and 203 m water depth at range 1000 m. The sound speed profile at vector sensor location is represented in Fig. 1 left showing a deep thermocline starting at depth 60 m. At deeper locations the sound speed profile was linearly extrapolated. The bottom was modeled as an half-space characterized by the values estimated in [10], bottom compressional speed of 1575 m/s, density of 1.5 g/cm³ and attenuation of 0.6dB/λ. The channel pressure and particle velocity field (horizontal and vertical components) frequency response were modeled by the CTRACEO ray tracing model [10]. The time domain received waveforms were synthesized by Fourier synthesis. Figure 2 shows the eigenrays (paths of the echoes that impinge the receiver) when the source is at 900 m (a), and the arrival patterns for the pressure (b), horizontal (c) and vertical (d) particle velocity. The arrival patterns for the pressure are normalized by the overall maximum, whereas the arrival patterns for the particle velocity components are normalized by the join overall maximum. Note that scale used for particle velocity arrival patterns are different. In the eigenrays plot, one can notice a direct echo and a surface reflected echo, which correspond to the earliest peaks in the arrival patterns plots. These echoes have small angles regarding the horizontal plane containing the source, decreasing with increasing source-receiver range. This behavior is observed in particle velocity components, specially in the vertical component, where the amplitude of peaks in the first cluster decreases as the source goes far-way from the receiver.

The latter echoes are bottom reflected. These echoes are also clustered in groups of 2 echoes depending on the number of surface reflections. Bottom reflected echoes have wider angles and lower amplitudes (pressure) mainly due to the attenuation in bottom. Note that in the vertical particle velocity arrival patterns the latter peaks have higher amplitudes since the angles are closer to the perpendicular. The amplitudes of the different echoes as seen by the vector sensor components illustrates in the time domain the spatial filtering capabilities of a single vector sensor. Table 1 presents the angles of the 4 earliest echoes impinging the vector sensor at different source distances, predicted by the forward model (*Fwd* label in SNR column) and estimated considering a SNR of 20, 5 and 0 dB. In order to attain a suitable amplitude and time delay resolution of the estimates, the sampling frequency of the received waveforms (48 kHz) were increased by a factor of 8.

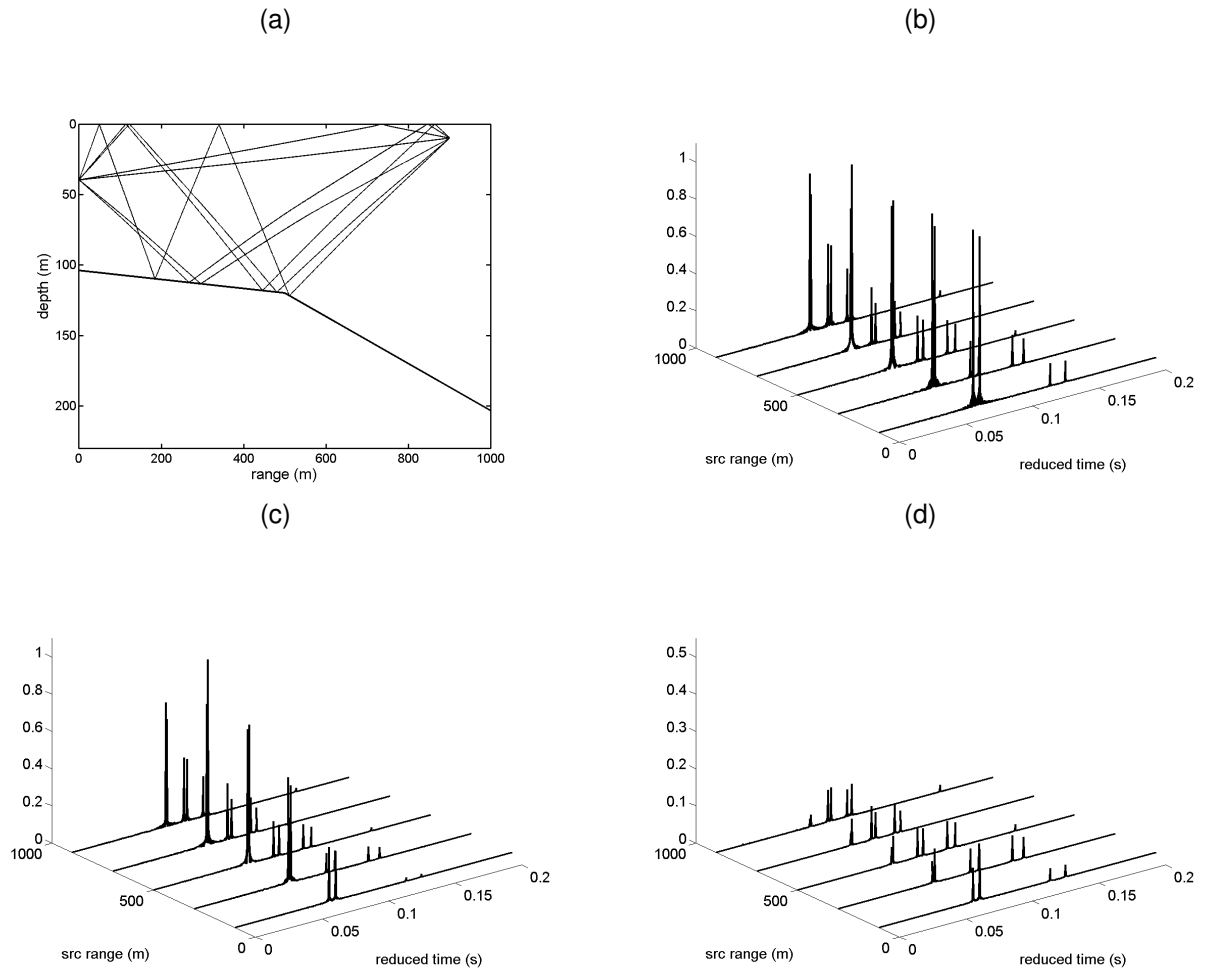


Figure 2: Eigenrays for a source at 900 m and arrival patterns for various source ranges – pressure (a), horizontal particle velocity (b), vertical particle velocity (c)

distance (m)	SNR (dB)	echo number			
		1	2	3	4
100	Fwd	16.3	26.1	-60	-63
	20	17.3	27.3	-59.2	-62.5
	5	17.5	27.2	-59.4	-62.8
	0	17.8	27.4	-56.0	-63.6
300	Fwd	5.6	9.3	-30.8	-33.8
	20	5.9	9.9	-31.8	-34.5
	5	5.8	9.9	-31.5	-34.6
	0	6.2	9.9	-30.8	-34.7
500	Fwd	3.3	5.5	-20.7	-22.8
	20	3.7	5.8	-21.8	-23.9
	5	3.6	5.9	-22.0	-24.0
	0	3.7	5.7	-21.8	-22.7
700	Fwd	2.3	3.9	-15.9	-17.6
	20	2.5	4.1	-16.8	-18.7
	5	2.6	4.1	-16.6	-18.8
	0	2.3	4.1	-17.0	-18.0
900	Fwd	1.8	2.9	-13.2	-14.5
	20	1.9	3.2	-14.1	-15.3
	5	1.8	3.2	-14.1	-15.2
	0	2.4	2.9	-14.0	-15.7

Table 1: Angles of the 4 earliest echoes impinging the vector sensor at different source distances as predicted by the forward model (Fwd) and estimated considering a SNR of 20, 5 and 0 dB

The table shows that the angle separation within a cluster of echoes decreases with increasing range, thus the estimation error should increase because real signals are band limited giving rise to higher interference between closer arrivals. Moreover, generally the signal to noise ratio at the receiver for distant signals decreases, that in turn also contributes to a higher estimates error at longer distances. Next simulation results are only for 900 M, the longer distance considered in this work, that should represent the worst case. Generally one can expect that the variance of angles related to latter arrivals should increase since those echoes are highly attenuated, thus in forthcoming results it is considered only the cases when 2 or 4 echoes are available. Figure 3(a) presents the backpropagated rays, which do not intercept at a single point due to angle and travel time estimation errors. The objective function dependence in range is plotted in lower figures for 4 echoes (b) and 2 echoes respectively. The estimated source range is given by the minimum of the objective function and corresponding depth in upper figure. One can notice errors bellow 50m in range and 2 m in depth for both the considered cases. When only two rays are backpropagated one can notice a increased ambiguity, specially in ranges close to the receiver, because of very short relative time delay between arrivals and close shooting angles.

However in the considered cases the source range-depth localization was attained with a small estimation error.

5 CONCLUSIONS

This paper illustrates by simulation the spatial filtering capability of a vector sensor applied to a broadband signal. It was shown the possibility of estimating the angle of arrival (elevation) of a single echo in a multipath environment. Given the estimates of the different echoes it was presented a method to estimate the source depth localization using a backpropagation algorithm. In comparison other with model based methods discussed in literature for source localization using a single device (hydrophone), the present method explores the spatial filtering capabilities of a single vector sensor to

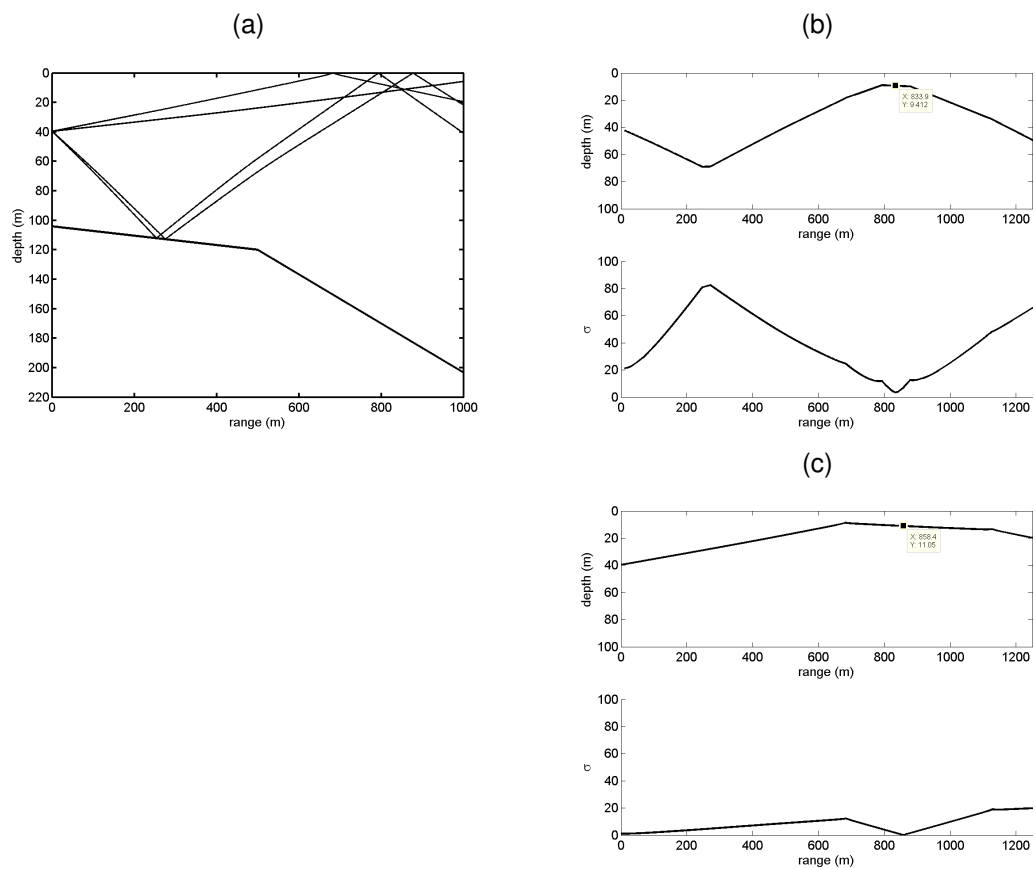


Figure 3: Backpropagated rays(a), ambiguity curves and source-localization plot using 4 rays (b) and 2 rays (c)

significantly reduce the number of forward model runs, thus it can be potentially used in real time systems.

ACKNOWLEDGEMENTS

This work was funded by National Funds through FCT- Foundation for Science and Technology under project SENSOCEAN (PTDC/EEA-ELC/104561/2008).

REFERENCES

1. J.-P. Hermand. Broad-band inversion in shallow water from waveguide impulse response measurements on a single hydrophone: theory and experimental results. *IEEE J. Oceanic Eng.*, 24(1): pp. 41–66, January 1999.
2. S. Jesus, M. Porter, Y. Stéphan, X. Démoulin, O. Rodriguez, and E. Coelho. Single hydrophone source localization. *IEEE J. Oceanic Eng.*, 25(3): pp. 337–346, July 2000.
3. J.-C. L. Gac, M. Asch, Y. Stéphan, and X. Démoulin. Geoacoustic inversion of broadband acoustic data in shallow water on a single hydrophone. *IEEE J. Oceanic Eng.*, 28(3): pp. 479–493, July 2003.
4. P. Felisberto, S. M. Jesus, Y. Stephan, and X. Demoulin. Shallow water tomography with a sparse array during the intimate'98 sea trial. In *Proc. MTS/IEEE Oceans'2003*, San Diego (USA), September 2003.
5. A. Nehorai and E. Paldi. Acoustic vector-sensor array processing. *IEEE Trans. Signal Processing*, 42(9): pp. 2481–2491, September 1994.
6. P. Felisberto, P. Santos, and S. M. Jesus. Tracking source azimuth using a single vector sensor. In *Proc. Int. Conf. on Sensor Technologies and Applications (SENSORCOMM 2010)*, Venice (Italy), July 2007.
7. M. Hawkes and A. Nehorai. Wideband source localization using a distributed acoustic vector-sensor array. *IEEE Trans. Signal Processing*, 27(3): pp. 628–637, July 2002.
8. P. Voltz and I.-T. Lu. A time-domain backpropagating ray technique for source localization. *J. Acoust. Soc. Am.*, 95(2): pp. 805–812, February 1994.
9. P. Santos, P. Felisberto, S. M. Jesus, and J. João. Geometric and seabed parameter estimation using a Vector Sensor Array –Experimental results from Makai experiment 2005. In *Proc. OCEANS'11*, Santander, Spain, June 2011.
10. P. Santos, O. C. Rodriguez, P. Felisberto, and S. M. Jesus. Seabed geoacoustic characterization with a vector sensor array. *Journal of the Acoustical Society of America*, 128(5): pp. 2652–2663, November 2010.